energy&fuels

Article

pubs.acs.org/EF

In-Depth Investigation of Chemical Looping Combustion of a Chinese Bituminous Coal with $CuFe_2O_4$ Combined Oxygen Carrier

Baowen Wang,*[,†,‡,∥] Weishu Wang,[†] Qiang Ma,[†] Jun Lu,[§] Haibo Zhao,[∥] and Chuguang Zheng[∥]

[†]College of Electric Power, North China University of Water Resources and Electric Power, Zheng Zhou 450045, China

[‡]Key Laboratory of Energy Thermal Conversion and Control of Ministry of Education, Southeast University, Nanjing 210096, China

[§]Xi'an Thermal Power Research Institute, Xi'an 710054, China

[∥]State Key Laboratory of Coal Combustion, Huazhong University of Science and Technology, Wuhan 430074, China

ABSTRACT: Coal is of heterogeneous nature with a complex chemical structure, which is closely associated with its reactivity. In this research, from the perspective of the chemical structure of coal, reaction characteristics of the as-synthesized $CuFe_2O_4$ oxygen carrier (OC) with a typical Chinese bituminous coal (designated as LZ) were deeply investigated using thermogravimetric analysis (TGA). Also, the effect of $CuFe_2O_4$ oxygen excess number Φ on the reaction behavior of LZ coal with $CuFe_2O_4$ was highlighted. TGA investigation of LZ coal reaction with $CuFe_2O_4$ at Φ = 1.0 displayed the enhanced reactivity of $CuFe_2O_4$, which was useful to conversion of the aromatic matrix in LZ coal. Furthermore, during LZ coal reaction with $CuFe_2O_4$ in the TGA, the gaseous products evolved from the condensed flue gas were in situ analyzed using Fourier transform infrared (FTIR), which indicated that most of the CO_2 resulted from oxidation of CO by $CuFe_2O_4$ OC. Meanwhile, the solid product left after LZ coal reaction with $CuFe_2O_4$ was analyzed with X-ray photoelectron spectroscopy (XPS), which revealed that oxidation and conversion of the C−C/C−H groups was the limited step at the molecular scale for full conversion of coal. Finally, the effect of $CuFe_2O_4$ excess number Φ for LZ coal reaction with $CuFe_2O_4$ was investigated by TGA, and the solid product left was analyzed by XPS, which indicated that C−C/C−H was more effectively converted at $CuFe_2O_4$ Φ = 1.0 than Φ = 0.5 and 1.5 at the final reaction temperature of 900 °C. In addition, the mechanism of coal oxidation by $CuFe_2O_4$ was also explored, and the C−C/C−H involved in LZ coal was preferentially oxidized to form C−O groups and then further converted to O═C−O groups through the formed intermediate C═O groups. Overall, this research was much beneficial for a mechanistic understanding of the conversion of coal in a CLC system and promotion of the efficient utilization of coal.

1. INTRODUCTION

Currently, capture and abatement of CO_2 emission from coal combustion is considered as one of the prime tasks to combat the aggravating greenhouse effect and global warming. Among various technologies available, chemical looping combustion (CLC) has been acknowledged as one of the novel combustion technologies for effective capture of the CO_2 without great energy penalty on the condition that continual use of coal as fuel for energy supply is sustained.[1]

With the present development of CLC technology, direct use of coal as fuel is considered as more advantageous for CLC application than syngas as fuel derived from gasification of coal.[2] So far, various fluidized bed rector systems have been operated for CLC with coal as fuel, and the capacities range from lab-scale to a 1 MW_{th} pilot plant.[3−10] All of these extensive experimental investigations have confirmed the feasibility of direct use of coal as fuel in a CLC system, but full conversion of residual char is determined as the limiting step and resists the full conversion of coal. To accelerate the char conversion and promote full reaction of coal with OC, most attention has been dedicated to this end and various factors are considered, including FR temperature,[3,4,11] system pressure,[5,7,12] mass ratio of OC to coal,[6,13,14] types and concentration of the gasifying agents such as CO_2 and steam,[15,16] and so on. Although all of these measures proved effective to some degree in the promotion of char conversion and its further reaction with OC, full conversion of coal was still not completely solved, which would result in many detrimental effects for economical operation of a CLC system and effective capture of CO_2.[17] Therefore, a more in-depth investigation of coal during CLC process should be made.

Coal is known as being of heterogeneous nature with a complex chemical structure, which is closely related to its reactivity.[18−20] Although coal has been utilized as one of the primary energy media for a long time, detailed characterization of the chemical structure of coal and its evolution during different thermal conversion processes is still a great challenge. Relative to various chemical approaches to characterize coal through thermal degradation,[21] direct characterization of coal chemical structure with nondesctructive approaches is more attractive.[18] Among various direct approaches, X-ray photoelectron spectroscopy (XPS) has been widely used to determine the elemental composition and chemical state of coal.[22] Furthermore, extra insight into the chemical structure of coal through different thermal conversion processes was gained, such as pyrolysis,[23] gasification,[24] low temperature oxidation,[25] and combustion,[26,27] which would be useful for thermal utilization of coal.

Yet different from investigation of the chemical structure of coal surviving these thermal processes, during CLC of coal,

Received: November 5, 2015
Revised: February 16, 2016
Published: February 17, 2016

DOI: 10.1021/acs.energyfuels.5b02605
Energy Fuels 2016, 30, 2285−2294

Table 1. Properties of LZ Coal Sample Studied

proximate analysis[a] (wt %)				ultimate analysis (wt %, ad[b])					
M_{ad}	V_{ad}	A_{ad}	FC_{ad}	C	H	N	S	O[c]	LHV[d] (MJ/kg)
0.54	16.82	41.88	40.76	41.07	1.81	0.85	5.23	8.67	23.354

ash analysis of LZ (wt %)									
SiO_2	Al_2O_3	Fe_2O_3	SO_3	CaO	TiO_2	Co_3O_4	K_2O	MgO	Na_2O
41.30	24.07	17.00	4.60	3.12	2.80	2.02	1.41	1.58	0.63

[a]M, moisture content; V, volatile matters; A, ash content; FC, fixed carbon; ad, air-dried basis. [b]Dry basis. [c]O content was determined by difference. [d]Lower heating value.

chemical reaction processes occurring were more complex, including coal pyrolysis, char gasification, and their instaneous interaction with OC, and thus research on the chemical structure of coal during CLC process is quite limited. Our previous preliminary investigation[28] was made on the distribution and evolution of different carbon functional groups in coal during its reaction with $CoFe_2O_4$ OC, but a deeper investigation was still quite deficient. Therefore, to promote the full conversion of coal, further research should be made to illuminate the evolution of chemical structure of coal during the CLC process.

In our previous research on CLC of coal,[29−31] $CuFe_2O_4$ is found to be a competitive combined OC with great potential for the realistic CLC application for its great superiority over the single oxides such as CuO and Fe_2O_3,[29,30] good resistance to sintering,[30] and satisfactory fuel adaptability, especially for coals of higher ranks such as sub-bituminous coal and anthracite,[30] and even for petroleum coke of quite low reactivity.[31] Meanwhile, the transfer of oxygen involved in $CuFe_2O_4$ OC to coal over the different temperature ranges was diversified,[30] and this combined OC could not only transfer the lattice oxygen involved for oxidation of coal, but also emit O_2 for coal combustion, which was quite attractive for CLC application. Yet a deep research on the distribution and evolution of various carbon groups involved in coal during its reaction with $CuFe_2O_4$ OC was not touched upon before based on the chemical structure of coal. Thus, in-depth investigation into the evolution of chemical structure coal during its reaction with $CuFe_2O_4$ is sure to be useful to gain a mechanistic understanding of the conversion of coal in a CLC system and promotion of the efficient utilization of coal.

Therefore, in this research, a typical Chinese bituminous coal with both high sulfur and mineral contents was selected. Its reaction with $CuFe_2O_4$ combined OC was investigated using thermogravimetric analyzer (TGA)-Fourier transform infrared (FTIR) analysis. Meanwhile, the distribution and evolution of various carbon functional groups involved in the selected coal during its reaction with $CuFe_2O_4$ OC were further studied using X-ray photoelectron spectroscopy (XPS). In addition, the effect of $CuFe_2O_4$ oxygen excess number on the LZ coal conversion was further explored so as to utilize coal in a CLC system more efficiently.

2. EXPERIMENTAL PROCEDURES

2.1. Material Preparation and Characterization. Both $CuFe_2O_4$ combined OC and their two reference oxide CuO and Fe_2O_3 used in this research were prepared with a novel sol−gel combustion synthesis (SGCS) method, in which several optimized procedures were involved, as described in more detail elsewhere,[32] including mixing of solutions with different precursors such as commercial copper and iron hydrated nitrates and urea, gel preparation, ignition of the dried gel, and sintering of the as-prepared OC. Finally, the prepared OC samples were ground, sieved, and particles of 63−106 μm were collected for use.

Meanwhile, one of the typical Chinese bituminous coal was collected from LiuZhi district, Guizhou province, one of the major production areas of Chinese coal, and abbreviated as LZ below. The collected LZ coal sample then was desiccated overnight at 105 °C, and further processed. After grinding and sieving, the LZ coal particles within 63−106 μm were selected and airtightly stored for use. The proximate, ultimate properties, and ash components of this coal were analyzed and presented in Table 1. From this table, it was observed that LZ coal is of a typical bituminous coal with both sulfur and ash contents reaching up to 5.23 and 41.88 wt %, respectively, much higher than those average ash and sulfur contents in Chinese coal as reported around 23.4[33] and 1.32 wt %[34] by the air-dried basis. The high ash and sulfur contents in Chinese coal would bring about great environmental harm as fuel for energy supply. Therefore, use of LZ coal as fuel in this research is meaningful and has important implication for the realistic application of CLC with Chinese coal as fuel in a more environmentally benign mode.

2.2. Determination of the $CuFe_2O_4$ Oxygen Excess Number Φ for LZ Coal Sample. After OC synthesis and coal preparation as described above, both the synthesized OCs and the prepared LZ coal sample were accurately weighed and uniformly mixed in a laboratory mortar at the fixed mass ratio, which was determined according to the coal mass balance method described below.[30,31] First, on the basis of the ultimate and proximate analysis data of LZ coal provided in Table 1, the relative chemical formula of 1 kg of LZ coal was represented as $C_{19.9}H_{9.9}N_{0.35}S_{0.95}O_{2.97}$. Assuming that the stoichiometric oxidation of 1 kg of LZ coal with $CuFe_2O_4$ was reached with $CuFe_2O_4$ reduced to Cu and Fe_3O_4, the $CuFe_2O_4$ oxygen excess number Φ provided relative to the 1 LZ coal was defined as 1. As a result, the mass ratio of $CuFe_2O_4$ to LZ coal was so determined as 7.84. Similarly, mass ratios of $CuFe_2O_4$ to LZ coal at Φ = 0.5 and 1.5 were determined as 3.92 and 11.76, respectively, while for the two reference single oxides CuO and Fe_2O_3, their mass ratios to LZ coal were accordingly calculated as 3.47 and 20.93.

2.3. Experimental Methods. Temperature-programmed reaction of LZ coal with the synthesized $CuFe_2O_4$ at the different oxygen excess numbers (including Φ = 0.5, 1.0, and 1.5) was conducted in a simultaneous thermal analyzer (STA 409C, Netzsch Corp., Germany) in a pure N_2 atmosphere with its flow rate fixed at 80 mL/min. An about 15 mg mixture of LZ coal with $CuFe_2O_4$ at the different mass ratios as described above in section 2.2 was loaded to the ceramic pan of the TGA and heated from ambient to 900 °C at 25 °C/min, and the soaking period at this temperature was kept for 20 min so as to ensure the sufficient conversion of LZ coal. In addition, prior to the formal TGA analysis, proper sample mass and flow rate of the N_2 carrier gas were determined to make the experimental results reproducible.

Meanwhile, the gaseous products evolved from reaction of LZ coal with $CuFe_2O_4$ in the TGA were simultaneously transferred to the coupled FTIR spectrometer (EQUINOX 55, Bruker Corp., Germany) and then in situ detected therein. The gas transfer line was heated around 180 °C to avoid condensation of the steam involved. The scanning range of FTIR was fixed at 4000−500 cm^{-1}, while the resolution and sensitivity parameters were set at 4 cm^{-1} and 1, respectively.

DOI: 10.1021/acs.energyfuels.5b02605
Energy Fuels 2016, 30, 2285−2294

After the TGA-FTIR investigation of the thermal reaction behavior of LZ coal with $CuFe_2O_4$, their solid products were carefully collected. Also, the distribution of the chemical states and surface compositions of interest were scanned and analyzed using an XPS spectrometer (VG MultiLab 2000, Thermo Electron Corp., U.S.), which was equipped with a monochromatic Mg Kα source ($h\nu$ = 1253.6 eV) and a charge neutralizer. The spectrometer was operated at 300 W of X-ray source power in a narrow scanning mode. Also, the base pressure and pass energy were fixed at 5×10^{-8} Pa and 25 eV, respectively, for high scanning resolution. All of the binding energies as obtained for the elements of interest were referenced to the C 1s peak at 284.6 eV. Meanwhile, the XPS spectra of the studied species were further deconvoluted using the AVANTAGE software affiliated with the XPS spectrometer. The relative contents of the obtained species were further quantified on the basis of the area of each curve-fitted component.

3. RESULTS AND DISCUSSION

3.1. TGA Investigation of Reaction of LZ Coal with $CuFe_2O_4$ OC. The reaction of LZ coal with the synthesized $CuFe_2O_4$ at the oxygen excess number Φ = 1.0 under N_2 atmosphere was performed in the TGA at 25 °C/min. Both the weight loss (TG) and the corresponding differential weight loss rate (DTG) for reaction of LZ coal with $CuFe_2O_4$ are presented in Figure 1. Meanwhile, pyrolysis of LZ coal under N_2 atmosphere and its reaction with single reference oxides CuO and Fe_2O_3 at the oxygen excess number Φ = 1.0 are included as well.

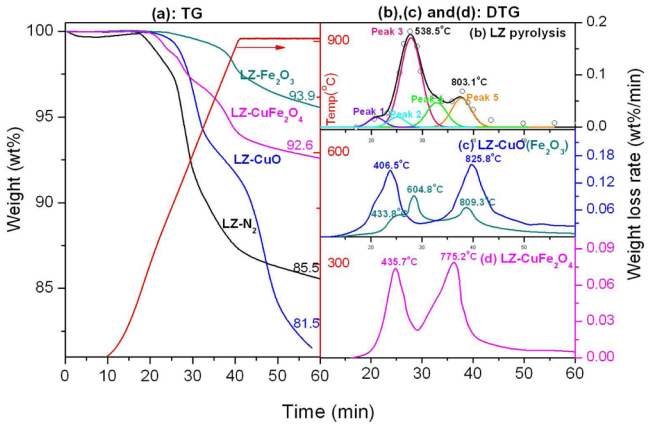

Figure 1. Reaction of LZ coal with $CuFe_2O_4$ OC at Φ = 1.0: (a) weight loss; (b) weight loss rate of LZ pyrolysis under N_2 atmosphere; (c) weight loss rate of LZ reaction with reference oxides CuO and Fe_2O_3; (and d) weight loss rate of LZ reaction with $CuFe_2O_4$ combined OC.

First, as a baseline, pyrolysis of LZ coal was conducted under N_2 atmosphere. Both TG and DTG data are presented in Figure 1a and b, respectively. It could be observed that after dehydration of the adsorbed water below 200 °C, two distinct reaction stages were observed.[35] The maximal DTG value at the first stage was around 0.1832 wt %/min, much higher than that value (0.0884 wt %/min) at the second stage. As accompanied by LZ pyrolysis and various light gases emitted, as shown in Figure 2a–d by gaseous FTIR analysis, numerous parallel and series reactions were reported to proceed simultaneously at the two reaction stages.[36] Also, cleavage of various covalent bonds and related functional groups present in LZ coal was involved.[37]

Furthermore, to learn the structure evolution of LZ coal during its pyrolysis process, according to the proposed bond dissociation energy (BDE) values,[37,38] the DTG curve of LZ pyrolysis was fitted into five reaction regions using a multiple Gaussian function, which was included in Figure 1b. Following other research,[39,40] these five regions were further assigned in the temperature ascending sequence as cleavage of weak bonds such as C_{al}–O bond at the peak temperature 383.2 °C for peak 1, relatively strong bonds such as C_{al}–C_{al}/C_{al}–H bond at 456.6 °C for peak 2, strong bonds such as C_{ar}–C_{al}/C_{ar}–O bond at 530.5 °C for peak 3, decomposition of carbonates especially calcite at 677.8 °C for peak 4, and condensation of aromatic carbon matrix at 816.3 °C for peak 5. According to the relative integrated areas of the five deconvoluted regions involved for LZ pyrolysis in Figure 1b, cleavage of C_{ar}–C_{al}/C_{ar}–O bond was identified as the biggest barrier for LZ pyrolysis other than the C_{al}–C_{al} reported by the Wei research group for Zhaotong lignite,[39] mainly due to the difference in the coal rank. In addition, the covalent bond in coal with the higher BDE value was known to crack at the higher temperature.[40] Therefore, cracking and condensation of the aromatic carbon matrix in LZ coal was most difficult among the whole pyrolysis of LZ coal, which was interesting and worth further exploration later.

As to the reaction of LZ coal with $CuFe_2O_4$ and its two reference oxides CuO and Fe_2O_3, their reaction behavior changed greatly, as shown in Figure 1a, c, and d. From the related TG curves shown in Figure 1a, the net final weight loss of LZ reaction with CuO was 18.5 wt %, much higher than that of LZ reaction with Fe_2O_3 (as 6.1 wt %), while for $CuFe_2O_4$ OC, its net final weight loss after reaction with LZ coal was 7.4 wt %, between those two net final weight losses of LZ coal with CuO and Fe_2O_3.

On the basis of the weight loss behaviors of $CuFe_2O_4$ OC and its two reference oxides CuO and Fe_2O_3 during reaction with LZ coal shown in Figure 1a, a parameter (α) for quantitative evaluation of the reactivity of $CuFe_2O_4$, CuO, and Fe_2O_3 during their reaction with LZ coal was developed from the previous research:[13]

$$\alpha = \frac{W_0 - W}{(f/(1+f))\Delta W_{OC} + (1/(1+f))\Delta W_{coal}} \quad (1)$$

where α is denoted as the conversion of $CuFe_2O_4$ OC or its two reference oxides CuO and Fe_2O_3 with LZ coal, and W_0 and W were the initial and instantaneous weight losses during reaction of $CuFe_2O_4$ OC or its two reference oxides with LZ coal (wt %), respectively. ΔW_{OC} and ΔW_{coal} referred to the maximal weight losses of OC and LZ coal, respectively, and f represented the mass ratio of $CuFe_2O_4$ OC, CuO, and Fe_2O_3 to LZ coal at their oxygen excess number Φ = 1, as defined in section 2.2. According to eq 1, the conversions of Fe_2O_3, $CuFe_2O_4$, and CuO during their reaction with LZ coal were calculated as 33.39%, 40.05%, and 64.78%, respectively, which indicated better reactivity of CuO with LZ coal than that of Fe_2O_3, and enhanced reactivity of the $CuFe_2O_4$ was also reached relative to Fe_2O_3, although still lower than that of CuO. Therefore, to overcome the limitation of CuO for its low melting point and inferior resistance to sintering and improvement of the reactivity of Fe_2O_3, the combined $CuFe_2O_4$ OC should be an interesting solution.

Finally, from Figure 1c and d for DTG curves of LZ coal reaction with the two reference oxides CuO, Fe_2O_3, and their combined $CuFe_2O_4$, it could be observed that far different from pyrolysis of LZ coal, the maximal DTG values at the second stage above 770 °C for reaction of LZ coal with CuO, Fe_2O_3,

DOI: 10.1021/acs.energyfuels.5b02605
Energy Fuels 2016, 30, 2285–2294

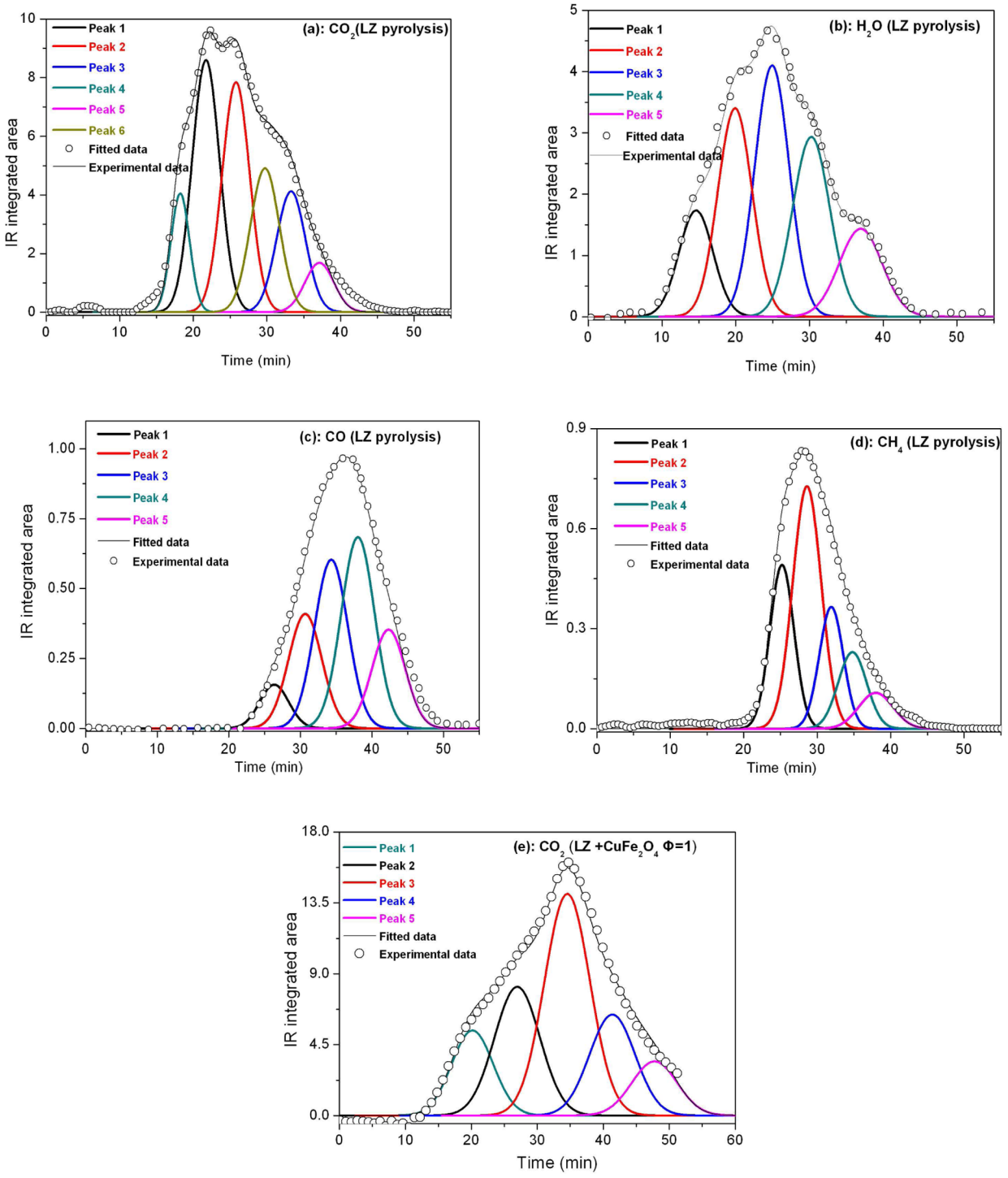

Figure 2. Main gaseous products evolved from LZ pyrolysis and its reaction with $CuFe_2O_4$ OC at Φ = 1.0: (a) CO_2 emitted from LZ pyrolysis; (b) H_2O evolved from LZ pyrolysis; (c) CO evolved from LZ pyrolysis; (d) CH_4 evolved from LZ pyrolysis; and (e) CO_2 evolved from reaction of LZ coal with $CuFe_2O_4$.

and $CuFe_2O_4$ improved greatly relative to those DTG values at the first stage, which indicated that addition of $CuFe_2O_4$ or their reference oxides was beneficial to conversion of the aromatic carbon matrix in LZ coal, as revealed in Figure 1b. In addition, it was noted that the two DTG maximal values for $CuFe_2O_4$ with LZ coal at the two reaction stages were lower than those of CuO with LZ coal, and the peak temperature gap between the two DTG maximal values for LZ coal with $CuFe_2O_4$ was only 339.5 °C, also much lower than that of LZ coal with CuO as 419.3 °C, which implied a higher oxygen transfer rate of $CuFe_2O_4$ during its reaction with LZ coal than that of CuO. Thus, it was reasonably inferred that a shorter duration of OC was needed at the fuel reactor of a CLC system to full conversion of coal with $CuFe_2O_4$.[41] In this way, $CuFe_2O_4$ should be preferred in the realistic CLC system over CuO or Fe_2O_3 for more economical operation.

3.2. FTIR Analysis of Gaseous Products Distribution during LZ Reaction with $CuFe_2O_4$. To further learn the

DOI: 10.1021/acs.energyfuels.5b02605
Energy Fuels 2016, 30, 2285−2294

Table 2. FTIR Peaks for the Characteristic Temperature of the Main Gaseous Products of Pyrolysis of LZ Coal and Its Further Reaction with $CuFe_2O_4$ OC

sample	gaseous products	characteristic temperature (°C)/T_x[a]							
LZ pyrolysis	CO_2		peak 1	peak 2	peak 3	peak 4	peak 5	peak 6	
			$240_{12.90}$	$355_{27.55}$	$473_{25.13}$	$585_{15.74}$	$690_{13.21}$	$790_{5.39}$	
	H_2O	peak 1	peak 2		peak 3	peak 4		peak 5	
		$130_{12.18}$	$297_{23.90}$		$452_{28.82}$	$603_{22.40}$		$793_{12.68}$	
	CO				peak 1	peak 2	peak 3	peak 4	peak 5
					$488_{6.23}$	$614_{18.72}$	$720_{27.60}$	$825_{31.28}$	$\sim 900_{16.15}$
	CH_4				peak 1	peak 2	peak 3	peak 4	peak 5
					$456_{22.93}$	$554_{40.17}$	$650_{17.04}$	$733_{12.68}$	$825_{7.17}$
LZ + $CuFe_2O_4$	CO_2			peak 1	peak 2		peak 3	peak 4+peak 5	
				$308_{14.6}$	$502_{22.1}$		$726_{38.0}$	$\sim 900_{25.14}$	

[a]Subscript numbers below the peak characteristic temperature T represent the relative percentage content of related functional groups.

distribution of gaseous products and ascertain the transformation of various related functional groups in LZ coal during its reaction with $CuFe_2O_4$ OC, gaseous products evolved from both pyrolysis of LZ coal and its reaction with $CuFe_2O_4$ in the TGA were in situ detected through the coupled FTIR spectrometer. Evolution of the main gaseous products is presented in Figure 2 as a function of time through integration of each IR gaseous species over its specific IR wavenumber region.

Generally, the FTIR identified gases during coal pyrolysis were of different sources and much complex.[42] Thus, deconvolution of the FTIR integrated spectra profiles for different gases was conducted using multiple Gaussian functions, which are shown in Figure 2 as well. Meanwhile, it was known quite difficult to assign the related functional groups due to various factors involved, such as coal ranks, heating rates, pressures, experimental system, etc.[19] Therefore, some well-established trends were followed,[42,43] which made it possible to determine the relationship between the functional groups and the gaseous products evolved from LZ pyrolysis and its further reaction with $CuFe_2O_4$ OC. In addition, the relative content of various functional groups involved was quantified on the basis of their integrated areas and is listed in Table 2.

First, from Figure 2a–d for various gaseous FTIR spectra of LZ pyrolysis under N_2 atmosphere, the main gaseous products were identified as several oxygenated gases, including H_2O, CO_2, CO, and light hydrocarbon gas CH_4. The related gaseous IR profiles were complex with partial overlapping, and thus were resolved using the curve-fitting method to explore their different sources and evolution of the related functional groups involved. As shown in Figure 2a, the CO_2 IR profile was resolved into six peaks between 200 and 800 °C, which were assigned in the temperature ascending sequence to carboxylic groups (COOH) at the characteristic temperature around 240 °C for peak 1,[20,44] an aromatic CO_2 site around the characteristic temperature 355 °C for peak 2,[45] carboxylic acid salts or esters at the characteristic temperature 473 °C for peak 3,[45] and lactones at the different energetic sites around the characteristic temperature 585 and 790 °C for peak 4 and peak 6,[46] respectively. Peak 5 around 690 °C mainly resulted from decomposition of calcite, which was found to exist in LZ coal as the main carbonate species and was easy to decompose under N_2 atmosphere around 700 °C.[28] Furthermore, according to Table 2, among all of these functional groups involved for CO_2 yield, the aromatic site at the peak 2 was determined as the largest contributor and made up 27.55% of the total CO_2 yield. Carboxylic salts or esters at peak 3 were little next to that of peak 2.

Similar to CO_2, as shown in Figure 2b, H_2O was mainly produced within 100–800 °C and deconvoluted into five peaks, among which the first peak at the characteristic temperature 130 °C was attributed to the release of the adsorbed water,[47] while the second peak at the characteristic temperature 297 °C was mainly formed from the condensation of the adjacent carboxylic function group within the same temperature range of peak 2 for CO_2.[43] Yet as shown in Table 2, for peak 3 at 452 °C, peak 4 at 603 °C, and peak 5 at 793 °C, they mainly resulted from condensation of different phenol derivatives due to the different BDE values.[48,49] Of course, H_2O was also emitted above 450 °C from some chemically bonded water present in various minerals of LZ coal, such as kaolinite ($Al_2Si_2O_5(OH)_4$) and gypsum ($CaSO_4{\cdot}2H_2O$).[45]

For CO, as shown in Figure 2c, it was mainly produced at a high temperature above 600 °C, which was resolved into five peaks. As shown in Table 2, the first peak at the characteristic temperature 488 °C contributed only 6.23% of CO, while peak 2 at the characteristic temperature 614 °C was closely associated with peak 4 for CO_2 and H_2O, which mainly resulted from secondary pyrolysis of the tars evolved from LZ pyrolysis.[20,50] Yet peak 3, peak 4, and peak 5 of CO above 700 °C were mainly produced from different C–O groups, such as scission of the phenolic oxygen groups or cracking of various ether groups.[51]

Far different from those three oxygenated gases (including CO_2, H_2O, and CO) discussed above for pyrolysis of LZ coal, as shown in Figure 2d, CH_4 was mainly produced within 400–700 °C and resulted from various aliphatic groups present in LZ coals. It was further deconvoluted into five peaks, among which peak 1 at 456 °C was assigned to demethylation of methyl oxygen groups (CH_3O-),[19] and peak 2 at 554 °C to the splitting of the methyl groups from aromatic rings.[21] According to Table 2, peak 2 was identified as the biggest contributor with the relative percentage reaching 40.17% for CH_4 yield. Meanwhile, peak 3 at 650 °C was responsible for decomposition of ary methyl group.[52] Peak 4 at 733 °C was attributed to cracking of aromatic heterocyclic structures, which only contributed 12.68% of CH_4, and thus was not the main reaction type for CH_4 evolution during LZ pyrolysis. A similar conclusion was reached by Liu et al.[53] Finally, for peak 5 at the characteristic temperature of 825 °C, its contribution to CH_4 was the least around 7.7%, and could be neglected as compared to other aliphatic groups for CH_4 yield, as analyzed above.

DOI: 10.1021/acs.energyfuels.5b02605
Energy Fuels 2016, 30, 2285–2294

While for reaction of LZ coal with $CuFe_2O_4$ OC, after condensation of the steam, the main gaseous product involved was identified as CO_2, which was deconvoluted into five peaks as shown in Figure 2e. Besides that the contribution from the CO_2 directly evolved from pyrolysis of LZ coal around the peak temperature 308 °C as discussed above, the main contribution of CO_2 resulted from reaction of $CuFe_2O_4$ with gaseous combustible products such as CH_4 and CO. As shown in Table 2, peak 2 at the characteristic temperature 502 °C mainly resulted from reaction of $CuFe_2O_4$ with the gaseous mixture of CH_4 and CO in a similar temperature range discussed above. Yet above 700 °C, peak 3, peak 4, and peak 5 for CO_2 yield mainly arose from reaction of $CuFe_2O_4$ with CO, which evolved from various C−O groups in LZ coal, and their total contribution to CO_2 reached 63%. Therefore, evolution of various C−O groups during reaction of LZ coal with $CuFe_2O_4$ should be paid enough attention for full conversion of LZ coal during the CLC process.

3.3. Effect of the $CuFe_2O_4$ Oxygen Excess Number Φ on Its Reaction with LZ Coal. Full conversion of coal is always one of the research focuses for CLC application. Among various potential factors available to improve coal conversion, such as reaction temperature, system pressure, and OC excess number Φ as pointed out in the Introduction, according to our previous evaluation,[54] the effect of the OC excess number Φ on the coal conversion is determined as the most significant. Therefore, reaction characteristics of LZ coal with $CuFe_2O_4$ OC at the different excess numbers, including Φ = 0.5, 1.0, and 1.5, were further studied with DTG curves provided in Figure 3.

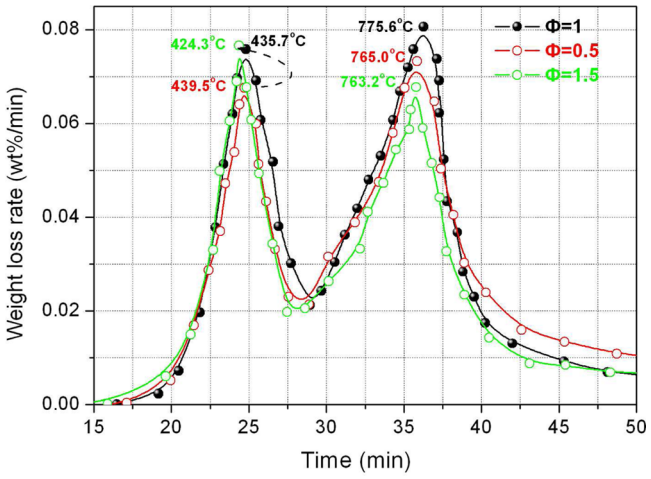

Figure 3. Effect of the different $CuFe_2O_4$ OC excess number Φ on its reaction with LZ coal.

From this figure, it could be observed that there existed two distinct reaction stages for reaction of LZ coal with $CuFe_2O_4$ at the different oxygen excess numbers. Reaction of $CuFe_2O_4$ with primary and secondary gaseous products from LZ coal was involved, as discussed above for Figure 1d. At the first stage, with the $CuFe_2O_4$ OC excess number Φ increasing from 0.5 to 1.5, a little decrease of the reaction characteristic temperature occurred for LZ coal with $CuFe_2O_4$ from 439.5 °C at Φ = 0.5 to 435.7 °C at Φ = 1.0 and further decreased to 424.3 °C at Φ = 1.5, but the maximal weight loss rate correspondingly increased from 0.0677 wt %/min at Φ = 0.5 to 0.0756 wt %/min at Φ = 1.0 and further to 0.0768 wt %/min at Φ = 1.5, which indicated that excess $CuFe_2O_4$ OC provided was always beneficial to coal conversion at the first reaction stage. Especially at the process from Φ = 0.5 to Φ = 1.0, introduction of more $CuFe_2O_4$ OC was favorable to coal conversion.

At the second reaction stage, the maximal reaction rate of LZ coal with $CuFe_2O_4$ at Φ = 1.0 reached 0.0807 wt %/min, which was the largest relative to those at Φ = 0.5 and Φ = 1.5, mainly due to the more adequate contact of the residual char left from pyrolysis of LZ coal with $CuFe_2O_4$ OC particles,[55,56] also similar to our previous finding for reaction of Fe_2O_3 with different coals.[57] In addition, the reaction characteristic temperature for LZ coal with $CuFe_2O_4$ at Φ = 1.0 was 775 °C, a little higher than those of LZ coal with $CuFe_2O_4$ at Φ = 0.5 and Φ = 1.5 with their characteristic temperatures centering around 760 °C. These characteristic temperatures were still much lower than the general operational temperature range for a realistic CLC application (850−950 °C). Therefore, reaction of LZ coal with $CuFe_2O_4$ at around Φ = 1.0 was more efficient for conversion of coal in a CLC system.

3.4. XPS Analysis of the Solid Products from Reaction of LZ Coal with $CuFe_2O_4$ OC. Variation in chemical structure of coal through direct oxidation by air at temperature lower than 400 °C has been widely investigated and found out as a complex process.[25,58] Yet oxidation of coal with $CuFe_2O_4$ OC during the CLC process at the temperature around 900 °C is more complex due to simultaneous occurrence of coal conversion, oxygen transfer from $CuFe_2O_4$ OC, and their interaction. Therefore, clarification of reaction of coal with $CuFe_2O_4$ OC from the chemical structural perspective is quite meaningful so as to gain an enhanced understanding for a more efficient conversion of coal in a CLC process.

3.4.1. Distribution and Evolution of Carbon Functional Groups in LZ Coal. Carbon is the dominant element in coal with its weight content changing due to the different coal rank.[59] As to LZ bituminous coal in this research, its XPS profiles in the C 1s region of 280−295 eV for the LZ original coal and its solid product left after reaction with $CuFe_2O_4$ are presented in Figure 4a and b, respectively. According to the well-established relationships between the C 1s binding energy (BE) values and the carbon functional groups involved,[60]

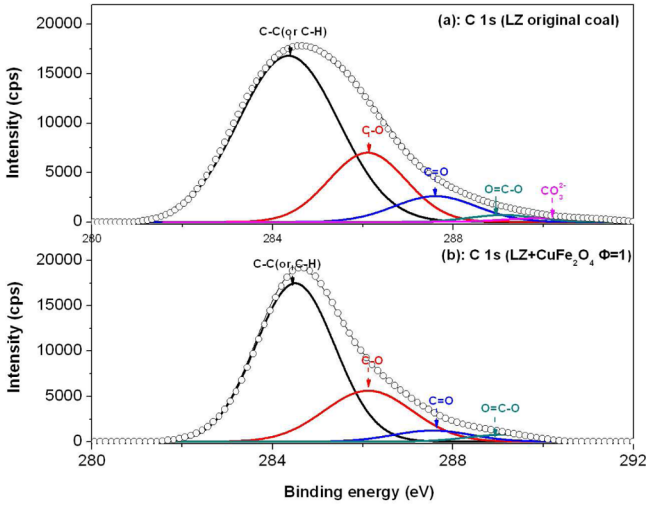

Figure 4. Distribution and evolution of carbon functional groups: (a) LZ original coal; and (b) LZ coal reaction with $CuFe_2O_4$ OC at Φ = 1.0.

DOI: 10.1021/acs.energyfuels.5b02605
Energy Fuels 2016, 30, 2285−2294

including 284.6 eV for aromatic and aliphatic carbon (C−C/C−H), 286.3 eV for carbon bound with one oxygen by a single bond (C−O), 287.5 eV for carbon bound to oxygen by two bonds (C═O), and 289.0 eV for carbon bound to oxygen by three bonds (O═C−O), the scanned C 1s regions were further curve-resolved into four main C 1s peaks using a mixed Gaussian−Lorentzian function. Meanwhile, another two carbon components were considered as well, including 290.5 eV for carbonates,[22] especially for calcite involved in the original LZ coal as verified in our previous research[28] and 291.5 eV for the $\pi-\pi^*$ shakeup from the contribution of the aromatic carbon matrix in coal.[61] Furthermore, as presented in Table 3, the relative carbon contents of different carbon functional groups were quantified on the basis of each deconvoluted XPS curve area.

Table 3. Relative Atomic Percentages of Various Carbon Functional Groups Present in LZ Coal and the Solid Products from Its Reaction with $CuFe_2O_4$ OC Determined by XPS Analysis

	relative content of carbon species (%)				
sample	C−C/C−H	C−O	C═O	COO^-	carbonates
LZ coal	71.23	11.90	11.60	1.41	3.87
LZ + $CuFe_2O_4$	57.26	31.72	7.95	3.07	N.A.

From Figure 4a for LZ original coal, its C 1s envelope was resolved into five carbon functional groups as C−C/C−H, C−O, C═O, O═C−O, and calcite (CO_3^{2-}). As shown in Table 3, their relative atomic contents were quantified as 71.23%, 11.90%, 11.60%, 1.41%, and 3.87%, respectively. Among these carbon functional groups, the content of the aromatic/aliphatic carbon (C−C/C−H) groups was determined as the dominant[62] and should be paid enough attention for sufficient conversion of coal.

Yet after reaction of LZ coal with $CuFe_2O_4$ at Φ = 1.0 by temperature-programmed heating from ambient to the prescribed 900 °C for 20 min, as shown in Figure 4b, the main C 1s envelope is more asymmetric toward higher binding energy with more oxygen incorporated into the main carbon matrix of LZ coal. This C 1s envelope was further deconvoluted into four peaks with exclusion of the CO_3^{2-} peak for its full decomposition and disappearance at relevant temperature in a CLC system.[28] As compared to those carbon functional groups of LZ coal shown in Figure 4a, the aromatic/aliphatic C−C/C−H group decreased a lot from 71.23% in LZ original coal to 57.26% by oxidation with $CuFe_2O_4$ OC at Φ = 1.0. Especially for aliphatic carbon groups (C−H) involved in LZ coal, they are reported as more sensitive to oxidation to form hydroxyl groups[63] and released as H_2O.[64]

Accompanied by the decline of the content of C−C/C−H groups, more C−O groups were preferred to formation with their relative content increasing a lot from 11.90% to 31.72% by nearly 3 times.[62] Similar to C−O groups, the relative content of O═C−O groups was also remarkably increased from 1.41% in LZ coal to 3.07% by nearly 3 times. Considering that O═C−O groups were considered as the main CO_2 precursor and easily decomposed at such a high temperature of 900 °C in this research,[45,46] a nearly triple increase of O═C−O groups implied that part of the formed C−O groups were eventually converted to O═C−O groups, as Gong et al.[25] and Wang et al.[62] proposed. Yet different from those two C−O and O═C−O groups, the relative content of C═O groups fell from 11.60% in LZ coal to 7.95%, similar to oxidation of Illinois No. 6 bituminous coal,[65] mainly because C═O groups were represented as the main intermediate product during coal oxidation by $CuFe_2O_4$ OC to form the O═C−O groups, on the one hand,[25,62] and also further disintegrated to emit CO, on the other hand,[20,50] as discussed in section 3.1.

3.4.2. Distribution of the Oxygen Species in LZ Coal and $CuFe_2O_4$ OC. Besides carbon, oxygen is another abundant element in coal, only next to carbon,[66] as validated from Table 1 for the ultimate analysis of LZ coal, which is quite complicated to characterize due to the intrinsic heterogeneity.[67] The O 1s XPS envelope of LZ original coal was deconvoluted as shown in Figure 5a. It could be observed that the great

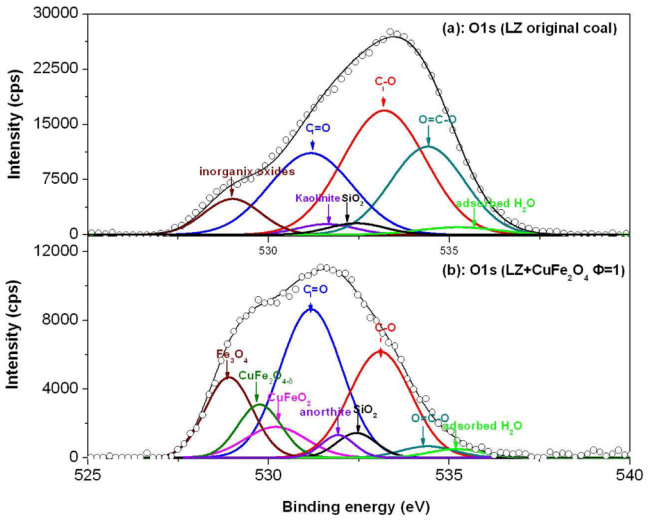

Figure 5. Distribution and evolution of various oxygen species: (a) LZ original coal; and (b) LZ coal reaction with $CuFe_2O_4$ OC LZ at Φ = 1.0.

contribution mainly resulted from various organic oxygen sources of C−O groups at the BE value ~532.9 eV, C═O groups at the BE value ~531.4 eV, and O═C−O groups at the BE value ~535.4 eV in LZ coal.[68,69] Meanwhile, inorganic oxygen sources from different minerals in LZ coal should be noted, mainly including some oxides, quartz (SiO_2), and kaolinite ($Al_2Si_2O_5(OH)_4$) as shown in Figure 5a. Especially for the latter two silicon-based minerals, they owned the propensity to enrich on the upper surface of coal particles[22] and overlapped with some organic oxygen functional groups (e.g., C═O groups, C−O groups) in a certain XPS regions,[70] which complicated identification and quantification of the related organic oxygen functional groups.

Yet after reaction of LZ coal with $CuFe_2O_4$, distribution of the oxygen species is more complex relative to the original coal. As shown in Figure 5b, besides the organic oxygen sources from those three oxygen functional groups involved in the residual char left after LZ coal reaction with $CuFe_2O_4$ OC, such as C−O, C═O, and O═C−O groups, the inorganic oxygen sources were more complex. On the one hand, $CuFe_2O_4$ OC was reduced during its reaction with LZ coal to form Fe_3O_4, $CuFeO_2$, and deficient $CuFe_2O_{4-\delta}$ ($0 \le \delta \le 2$). On the other hand, quartz of different crystalline was formed. Meanwhile, as shown in Figure 5b, interaction of minerals in LZ coal also occurred with anorthite ($CaAl_2Si_2O_8$) formed, which resulted from reaction of kaolinite with calcite ($CaCO_3$) on the surface

DOI: 10.1021/acs.energyfuels.5b02605
Energy Fuels 2016, 30, 2285−2294

of the solid products during reaction of LZ coal with $CuFe_2O_4$, as validated in our previous research.[71,72]

3.4.3. Distribution of the Reduced $CuFe_2O_4$ OC during Its Reaction with LZ Coal. Furthermore, to gain a deeper understanding on the evolution of $CuFe_2O_4$ OC during its reaction with LZ coal, XPS analysis of Cu and Fe species evolved from the reduced $CuFe_2O_4$ OC was further conducted and shown in Figure 6a and b, respectively. It was observed that

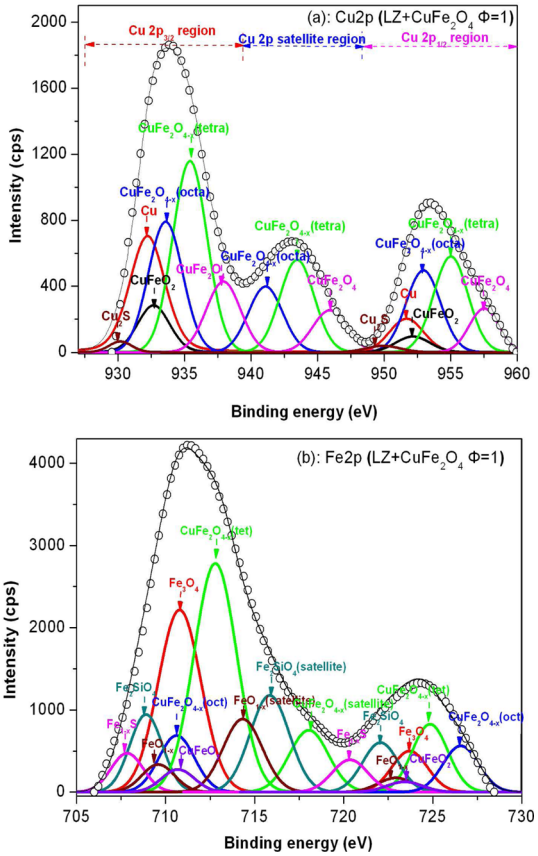

Figure 6. Distribution and evolution of the reduced $CuFe_2O_4$ OC during its reaction with LZ at Φ = 1.0: (a) Cu species; and (b)Fe species.

due to the spin−orbit doublet of Cu 2p and Fe 2p regions, the related regions were mainly separated into 2p 3/2 and 2p 1/2 parts. In combination with Figure 6a for Cu species and Figure 6b for Fe species, deficient $CuFe_2O_{4-\delta}$ ($0 \le \delta \le 2$) was found to form on the basis of the different characteristic Cu^{2+} and Fe^{3+} BE values.[73,74] More Cu^{2+} and Fe^{3+} ions were found to preferably occupy at the octahedral sites[75] instead of the tetrahedral sites in the $CuFe_2O_4$ OC and made the crystal structure of $CuFe_2O_4$ inverted, which mainly resulted from the reduction of $CuFe_2O_4$ by the gaseous pyrolysis products of LZ coal at the relatively low temperature.[30,31] This partially inverted structure was considered as beneficial to transfer the lattice oxygen[76] involved to oxidize LZ coal, which should be responsible for the higher oxygen transfer rate of $CuFe_2O_4$ than those CuO and Fe_2O_3, as shown in Figure 1d. Meanwhile, some $CuFeO_2$,[77] Cu,[78] and Fe_3O_4[79] were also identified to present according to their specific BE values, which were ascribed to the direct decomposition of $CuFe_2O_4$ at temperature higher than 800 °C by emission of O_2 and further transfer of the residual lattice oxygen involved for coal combustion, as validated in our previous investigation.[30,31]

In addition, as to Fe_2SiO_4 and Cu_2S, they were formed through interaction between the reduced $CuFe_2O_4$ counterparts with the silicon-based minerals and sulfur species evolved from LZ coal, respectively. Although these minor species were of great detrimental effects on the reactivity of $CuFe_2O_4$ OC and efficient conversion of coal, their formation was quite complex and out of the current research focus, which could be referenced elsewhere in our other research.[72,80]

3.4.4. Effect of the $CuFe_2O_4$ Excess Number Φ on the Evolution of Carbon Function Groups. Finally, although the effect of the OC excess number Φ on the conversion of coal in CLC has been widely investigated and identified as an effective measure to promote coal conversion,[54] research related to the effect of the oxygen excess number Φ on the evolution of different carbon functional groups in coal during CLC process was quite limited. Therefore, taking reaction of $CuFe_2O_4$ with LZ coal at the final temperature of 900 °C as an example in this research, the effect of $CuFe_2O_4$ excess number Φ on the evolution of four different carbon functional groups (including C−C/C−H, C−O, C═O, and O═C−O groups) involved in LZ coal was studied and shown in Figure 7a−d, respectively. Meanwhile, the relative contents of the four carbon functional groups for LZ original coals were included as well for comparison and designed as the case of Φ = 0.

From Figure 7a, it could be observed that relative to the fractions of the C−C/C−H groups in LZ original coal, with the $CuFe_2O_4$ oxygen excess number Φ increased from 0.5 to 1.5 and more $CuFe_2O_4$ OC introduced into LZ coal, the fraction of C−C/C−H groups decreased a lot from 71.23% in LZ original coal to 68.35% for LZ coal with $CuFe_2O_4$ at Φ = 0.5, further to 57.26% at Φ = 1.0, and to 55.56% at Φ = 1.5, respectively. More lattice oxygen of $CuFe_2O_4$ was incorporated into C═C/C−H groups of LZ coal, which resulted in more C−C/C−H groups converted to C−O groups, as discussed above. Especially, due to more effective contact of LZ coal char with $CuFe_2O_4$ OC at Φ = 1.0 and thus to enhance the transfer of oxygen in $CuFe_2O_4$ to LZ coal, a higher conversion rate of C−C/C−H to C−O groups in LZ coal was reached, as evidenced by the steeper slope shown in Figure 7a. In addition, although the increase of $CuFe_2O_4$ OC was always beneficial to conversion of C−C/C−H groups in LZ coal, oversupply of the $CuFe_2O_4$ OC for coal conversion was not economical for a realistic CLC system.

Accompanied by the decrease of C−C/C−H groups in LZ coal with more $CuFe_2O_4$ introduced as discussed above, as shown in Figure 7b and d, the increase of $CuFe_2O_4$ OC excess number Φ during reaction of LZ coal with $CuFe_2O_4$ was found evidently to increase the fraction of the C−O and O═C−O groups. Meanwhile, the fraction of C−O groups was dominated relative to those two C═O and O═C−O groups, mainly due to the preferential formation of C−O groups over C═O and O═C−O groups during reaction of LZ coal with $CuFe_2O_4$, as discussed in section 3.4.1. Yet contrarily, the fraction of C═O groups was always stabilized around 8% as shown in Figure 7c, which was due to the balance of the formation of C═O groups through conversion of C−O groups against the further conversion of C═O groups to solid O═C−O groups. Simultaneously, part of the C═O groups was disintegrated to CO.[25,62]

Overall, TG-FTIR analysis of LZ coal with $CuFe_2O_4$ OC from the related functional groups perspective was conducted

DOI: 10.1021/acs.energyfuels.5b02605
Energy Fuels 2016, 30, 2285−2294

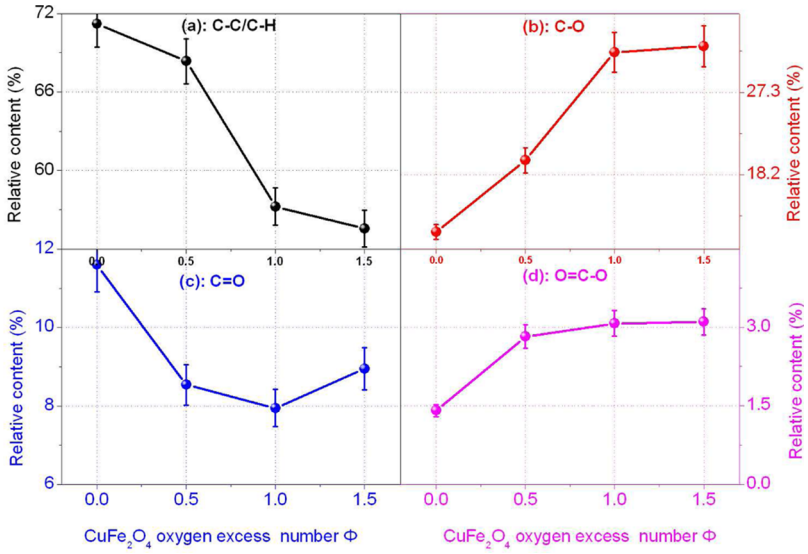

Figure 7. Effect of $CuFe_2O_4$ OC excess number Φ on the evolution of related carbon functional groups in LZ coal: (a) C−C/C−H groups; (b) C−O groups; (c) C═O groups; and (d) O═C−O groups.

in sections 3.1 and 3.2. Meanwhile, investigation of the distribution and evolution of the carbon functional groups in LZ coal was used by XPS. This comprehensive research was beneficial to gain an insightful understanding on the conversion of coal in CLC from the molecular scale, and would be also conducive to operation of a realistic CLC system with more efficient conversion of coal.

4. CONCLUSIONS

Reaction of $CuFe_2O_4$ with a typical Chinese bituminous coal was performed through TGA coupled with FTIR analysis, and then XPS characterization of the chemical structure of LZ coal during its reaction with $CuFe_2O_4$ was made. Meanwhile, the effect of the $CuFe_2O_4$ excess number Φ on its reaction with LZ coal and evolution of the carbon functional groups was studied in detail. Such conclusions were reached as follows:

(1) TGA analysis of $CuFe_2O_4$ reaction with LZ coal displayed the desired reaction superiority of $CuFe_2O_4$ with high reactivity and oxygen transfer rate for conversion of the aromatic carbon matrix in LZ coal.

(2) FTIR analysis of the gaseous products evolved from reaction of LZ coal with $CuFe_2O_4$ indicated that most of the formed CO_2 resulted from further oxidation of CO emitted from various C−O groups in LZ coal by $CuFe_2O_4$ OC.

(3) XPS analysis of the carbon functional groups present in the LZ coal and the solid product after its reaction with $CuFe_2O_4$ revealed that oxidation and conversion of the C−C/C−H groups was the limited step at the molecular scale for full conversion of coal.

(4) The oxidization mechanism of LZ coal with $CuFe_2O_4$ from the chemical structure perspective of coal was illuminated, and oxidation of C−C/C−H groups in LZ coal was preferentially converted to C−O groups, further to the intermediate C═O groups, and finally to O═C−O groups.

(5) TGA investigation on the effect of the $CuFe_2O_4$ excess number Φ as well as XPS analysis of the solid products left indicated that C−C/C−H was more effectively converted at $CuFe_2O_4$ Φ = 1.0 instead of Φ = 0.5 and 1.5.

AUTHOR INFORMATION

Corresponding Author

*Tel./fax: (371)69127630. E-mail: david-wn@163.com.

Notes

The authors declare no competing financial interest.

ACKNOWLEDGMENTS

This work is supported by the National Natural Science Foundation of China (nos. 51276210, 50906030), the Foundations of Key Laboratory of Energy Thermal Conversion and Control of Ministry of Education, Key R&D program of Henan Province, Innovative Research Team in S&T in University of Henan Province (16IRTSTHN017), and North China University of Water Resources and Electric Power (no. 70481). Meanwhile, the support provided by the China Scholarship Council (CSC 201508410060) is appreciated.

REFERENCES

(1) Adanez, J.; Abad, A.; Garcia-Labiano, F.; Gayan, P.; de Diego, L. F. *Prog. Energy Combust. Sci.* **2012**, *38*, 215−282.
(2) Cao, Y.; Pan, W.-P. *Energy Fuels* **2006**, *20*, 1836−1844.
(3) Berguerand, N.; Lyngfelt, A. *Fuel* **2010**, *89*, 1749−1762.
(4) Shen, L. H.; Wu, J. H.; Gao, Z. P.; Xiao, J. *Combust. Flame* **2010**, *157*, 934−942.
(5) Xiao, R.; Chen, L. Y.; Saha, C.; Zhang, S.; Bhattacharya, S. *Int. J. Greenhouse Gas Control* **2012**, *10*, 363−373.
(6) Yang, W. J.; Zhao, H. B.; Ma, J. C.; Mei, D. F.; Zheng, C. G. *Energy Fuels* **2014**, *28*, 3970−3981.
(7) Zhang, S.; Xiao, R.; Zheng, W. G. *Appl. Energy* **2014**, *130*, 181−189.
(8) Markström, P.; Linderholm, C.; Lyngfelt, A. *Int. J. Greenhouse Gas Control* **2013**, *15*, 150−162.
(9) Abad, A.; Pérez-Vega, R.; de Diego, L. F.; García-Labiano, F.; Gayán, P.; Adánez, J. *Appl. Energy* **2015**, *157*, 295−303.
(10) Ströhle, J.; Orth, M.; Epple, B. *Appl. Energy* **2015**, *157*, 288−294.
(11) Adánez-Rubio, I.; Gayán, P.; Abad, A.; García-Labiano, F.; de Diego, L. F.; Adánez, J. *Chem. Eng. J.* **2014**, *256*, 69−84.
(12) Xiao, R.; Song, Q.; Song, M.; Lu, Z.; Zhang, S.; Shen, L. *Combust. Flame* **2010**, *157*, 1140−1153.
(13) Sun, X. Y.; Xiang, W. G.; Wang, S.; Tian, W. D.; Xu, X.; Xu, Y. J.; Xiao, Y. H. *J. Therm. Sci.* **2010**, *19*, 266−275.

DOI: 10.1021/acs.energyfuels.5b02605
Energy Fuels 2016, 30, 2285−2294

(14) Dennis, J.; Scott, S. A. *Fuel* **2010**, *89*, 1623−1640.
(15) Shen, L. H.; Wu, J. H.; Xiao, J. *Combust. Flame* **2009**, *156*, 721−728.
(16) Scott, S. A.; Dennis, J. S.; Hayhurst, A. N. *AIChE J.* **2006**, *52*, 3325−3328.
(17) Lyngfelt, A. *Appl. Energy* **2014**, *113*, 1869−1873.
(18) Haenel, M. W. *Fuel* **1992**, *71*, 1211−1223.
(19) Van Heek, K. H.; Hodek, W. *Fuel* **1994**, *73*, 886−896.
(20) Niksa, S. *Energy Fuels* **1996**, *10*, 173−187.
(21) Hodek, W.; Kirschstein, J.; van Heek, K.-H. *Fuel* **1991**, *70*, 424−428.
(22) Perry, D. L.; Grint, A. *Fuel* **1983**, *62*, 1024−1032.
(23) Liu, F. R.; Li, W.; Guo, H. Q.; Li, B. Q.; Bai, Z. Q.; Hu, R. S. *J. Fuel Chem. Technol.* **2011**, *39*, 81−84.
(24) Domazetis, G.; Liesegang, J.; Jams, B. D. *Fuel Process. Technol.* **2005**, *86*, 463−486.
(25) Gong, B.; Pigram, P. J.; Lamb, R. N. *Fuel* **1998**, *77*, 1081−1087.
(26) Xian, J.; Hu, S.; Sun, L. S.; Xu, M. H.; Li, P. S.; Su, S.; Sun, X. X. *J. Chem. Ind. Eng. (China)* **2006**, *57*, 2180−2184.
(27) Zhang, Y. C.; Zhang, J.; Sheng, C. D.; Liu, Y. X.; Zhao, L.; Ding, Q. Z.; Wang, K. *Proc. Chin. Soc. Electr. Eng.* **2011**, *31*, 27−31.
(28) Wang, B. W.; Gao, C. C.; Wang, W. S.; Kong, F. H.; Zheng, C. G. *J. Anal. Appl. Pyrolysis* **2014**, *105*, 369−378.
(29) Wang, B. W.; Zheng, Y.; Liu, Z. H.; Zhao, H. B.; Zheng, C. G.; Yan, R. *J. Eng. Thermophys.* **2010**, *31*, 1427−1430.
(30) Wang, B. W.; Yan, R.; Zhao, H. B.; Zheng, Y.; Zheng, C. G. *Energy Fuels* **2011**, *25*, 3344−3354.
(31) Wang, B. W.; Zhao, H. B.; Zheng, Y.; Liu, Z. H.; Zheng, C. G. *Chem. Eng. Technol.* **2013**, *36*, 1488−1495.
(32) Wang, B. W.; Yan, R.; Lee, D. H.; Zheng, Y.; Zhao, H. B.; Zheng, C. G. *J. Anal. Appl. Pyrolysis* **2011**, *91*, 105−113.
(33) Sun, G. D. *Coal in China: Resources, Uses and Advanced Coal Technologies*; Pew Center on Global Climate Change: Arlington, VA, 2010; http://www.c2es.org/docUploads/coal-in-china-resources-uses-technologies.pdf.
(34) Tang, S. H.; Sun, S. L.; Qin, Y.; Jiang, Y. F.; Wang, W. F. *Acta Geol. Sin.* **2008**, *82*, 722−730.
(35) Yang, H. P.; Chen, H. P.; Ju, F. D.; Yan, R.; Zhang, S. H. *Energy Fuels* **2007**, *21*, 3165−3170.
(36) Burnham, A. K.; Oh, M. S.; Crawford, R. W.; Samoun, A. M. *Energy Fuels* **1989**, *3*, 42−55.
(37) Shi, L.; Liu, Q. Y.; Guo, X. J.; Wu, W. Z.; Liu, Z. Y. *Fuel Process. Technol.* **2013**, *108*, 125−132.
(38) He, Q. Q.; Wan, K. J.; Hoadley, A.; Yeasmin, H.; Miao, Z. Y. *Fuel* **2015**, *156*, 121−128.
(39) Li, Z.-K.; Wei, X.-Y.; Yan, H.-L.; Zong, Z.-M. *Fuel* **2015**, *153*, 176−182.
(40) Luo, Y. R. *Comprehensive Handbook of Chemical Bond Energies*; CRC Press: New York, 2007; pp 19−365.
(41) Mattisson, T.; Lyngfelt, A.; Cho, P. *Fuel* **2001**, *80*, 1953−1962.
(42) Figeeiredo, J. L.; Pereira, M. F. R.; Freitas, M. M. A.; Órfão, J. J. M. *Carbon* **1999**, *37*, 1379−1389.
(43) Szymański, G. S.; Karpiński, Z.; Biniak, S.; Świątkowski, A. *Carbon* **2002**, *40*, 2627−2639.
(44) Serio, M. A.; Hamblen, D. G.; Markham, J. R.; Solomon, P. R. *Energy Fuels* **1987**, *1*, 138−152.
(45) Giroux, L.; Charland, J.-P.; MacPhee, J. A. *Energy Fuels* **2006**, *20*, 1988−1996.
(46) Zhou, J.-H.; Sui, Z.-J.; Zhu, J.; Li, P.; Chen, D.; Day, Y.-C.; Yuan, W.-K. *Carbon* **2007**, *45*, 785−796.
(47) Wang, S. Q.; Tang, Y. G.; Schobert, H. H.; Guo, Y. N.; Gao, W. C.; Lu, X. K. *J. Anal. Appl. Pyrolysis* **2013**, *100*, 75−80.
(48) MacPhee, J. A.; Charland, J.-P.; Giroux, L. *Fuel Process. Technol.* **2006**, *87*, 335−341.
(49) Arenillas, A.; Rubiera, F.; Pis, J. J.; Cuesta, M. J.; Iglesias, M. J.; Jimenez, A.; Suarez-Ruiz, I. *J. Anal. Appl. Pyrolysis* **2003**, *68−69*, 371−385.
(50) Solomon, P. R.; Serio, M. A.; Carangelo, R. M.; Bassilakis, R.; Gravel, D.; Baillargeon, M.; Baudais, F.; Vail, G. *Energy Fuels* **1990**, *4*, 319−333.
(51) Liu, J. X.; Jiang, X. M.; Shen, J.; Zhang, H. *Energy Convers. Manage.* **2014**, *87*, 1039−1049.
(52) Arenillas, A.; Rubiera, F.; Pis, J. J. *J. Anal. Appl. Pyrolysis* **1999**, *50*, 31−46.
(53) Liu, J. X.; Jiang, X. M.; Shen, J.; Zhang, H. *Energy Convers. Manage.* **2014**, *87*, 1027−1038.
(54) Wang, B. W.; Zheng, Y.; Zhao, H. B.; Liu, Z. H.; Zheng, C. G. Simulated investigation of chemical looping combustion of coal with Fe-based combined oxygen carrier. *Chin. Soc. Eng. Thermophys. Conf.*; Guangzhou, China, 2010.
(55) Siriwardane, R.; Tian, H. J.; Miller, D.; Richards, G.; Simonyi, T.; Poston, J. *Combust. Flame* **2010**, *157*, 2198−2208.
(56) Piekiel, N. W.; Egan, G. C.; Sullivan, K. T.; Zachariah, M. R. *J. Phys. Chem. C* **2012**, *116*, 24496−24502.
(57) Wang, B. W.; Yan, R.; Zheng, Y.; Zhao, H. B.; Zheng, C. G. *Fuel* **2011**, *90*, 2359−2366.
(58) Liotta, R.; Brons, G.; Isaacs, J. *Fuel* **1983**, *62*, 781−791.
(59) Weitzsacker, C. L.; Gardella, J. A., Jr. *Energy Fuels* **1996**, *10*, 141−148.
(60) Kelemen, S. R.; Afeworki, M.; Gorbaty, M. L.; Cohen, A. D. *Energy Fuels* **2002**, *16*, 1450−1462.
(61) Kelemen, S. R.; Rose, K. D.; Kwiatek, P. J. *Appl. Surf. Sci.* **1993**, *64*, 167−173.
(62) Wang, H.; Dlugogorski, B. Z.; Kennedy, E. M. *Combust. Flame* **2003**, *134*, 107−117.
(63) Kalema, W. S.; Gavalas, G. R. *Fuel* **1987**, *66*, 158−164.
(64) Kims, S.; Zhou, S.; Hu, Y.; Acik, M.; Chabal, Y.; Berger, C. *Nat. Mater.* **2012**, *11*, 544−549.
(65) Kelemen, S. R.; Freund, H. *Energy Fuels* **1989**, *3*, 498−505.
(66) Kelemen, S.r.; Kwiaterk, P. J. *Energy Fuels* **1995**, *9*, 841−848.
(67) Dong, P. W.; Chen, G.; Zeng, X.; Chu, M.; Gao, S. Q.; Xu, G. W. *Energy Fuels* **2015**, *29*, 2268−2276.
(68) Pietrzak, R.; Grzybek, T.; Wachowska, H. *Fuel* **2007**, *86*, 2616−2624.
(69) Fiedler, R.; Bendler, D. *Fuel* **1992**, *71*, 381−388.
(70) Grzybek, T.; Kreiner, K. *Langmuir* **1997**, *13*, 909−912.
(71) Traoré, K.; Blanchart, P. *J. Mater. Res.* **2003**, *18*, 475−481.
(72) Wang, B. W.; Zhao, H. B.; Zheng, Y.; Liu, Z. H.; Yan, R.; Zheng, C. G. *Fuel Process. Technol.* **2012**, *96*, 104−115.
(73) Zhang, Y.; Wei, T. T.; Xu, K. Z.; Ren, Z. Y.; Xiao, L. B.; Song, J. R.; Zhao, F. Q. *RSC Adv.* **2015**, *5*, 75630−75635.
(74) Shimoda, N.; Faungnawakij, K.; Kikuchi, R.; Fukunaga, T.; Eguchi, K. *Appl. Catal., A* **2009**, *365*, 71−78.
(75) Reitz, C.; Suchomski, C.; Haetge, J.; Leichtweiss, T.; Jaglicic, Z.; Djerdj, I.; Brezesinski, T. *Chem. Commun.* **2012**, *51*, 4471−4473.
(76) Zhang, P.; Yu, B.; Zhang, L. *Sci. China, Ser. B: Chem.* **2009**, *52*, 101−108.
(77) Chen, H.-Y.; Wu, J.-H. *Thin Solid Films* **2012**, *520*, 5029−5035.
(78) Biesinger, M. C.; Lau, L. W. M.; Gerson, A. R.; Smart, R.St.C. *Appl. Surf. Sci.* **2010**, *257*, 887−898.
(79) Paparazzo, E. *Surf. Interface Anal.* **1988**, *12*, 115−118.
(80) Wang, B. W.; Gao, C. C.; Wang, W. S.; Zhao, H. B.; Zheng, C. G. *J. Environ. Sci.* **2014**, *26*, 1−9.

DOI: 10.1021/acs.energyfuels.5b02605
Energy Fuels 2016, 30, 2285−2294